Time Separation Technique Using Prior Knowledge for Dynamic Liver Perfusion Imaging

Hana Haseljić[a], Vojtěch Kulvait[b], Robert Frysch[a], Fatima Saad[a], Bennet Hensen[c], Frank Wacker[c], Inga Brüsch[d], Thomas Werncke[c], and Georg Rose[a]

[a]Institute for Medical Engineering and Research Campus STIMULATE, Otto-von-Guericke University, Magdeburg, Germany
[b]Institute of Materials Physics, Helmholtz-Zentrum hereon, Geesthacht, Germany
[c]Institute of Diagnostic and Interventional Radiology, Hannover Medical School, Hannover, Germany
[d]Institute for Laboratory Animal Science, Hannover Medical School, Hannover, Germany

ABSTRACT

The perfusion imaging using C-arm CT could be used intraoperatively for liver cancer treatment planning and evaluation. To deal with undersampled data due to slow C-arm CT rotation and pause between the rotations, we applied model-based reconstruction methods. Recent works using the time separation technique with an analytical basis function set have led to a significant improvement in the quality of C-arm CT perfusion maps. In this work we apply the time separation technique with a prior knowledge basis function set extracted using singular value decomposition from CT perfusion reconstructions. On C-arm CT liver perfusion scan simulated based on the real CT liver perfusion scan we show that the bases extracted from only two CT perfusion scans are capable of modeling the C-arm CT data correctly.

Keywords: dynamic perfusion imaging, C-arm CT, prior knowledge, singular value decomposition

1. INTRODUCTION

CT imaging is an important step in liver cancer therapy planning, see 1. The C-arm CT perfusion imaging could interventionally assist in the cancer treatments by offering the possibility to evaluate the success of performed embolization or in ablation planning. The so far investigated protocols for estimation of parenchymal blood flow, see 2–4, would not be sufficient to capture the dynamic perfusion, so ten sweep perfusion protocol was suggested in 5. However, the problem of undersampled data due to limited number of projections per rotation and pause times between in between remain. In 6 it was shown that the model-based reconstruction by applying Time separation technique (TST) with analytical basis function set could solve these problems. The possibility to use dedicated, so called prior knowledge, basis function set formed from singular vectors extracted by applying singular value decomposition (SVD) to CT perfusion reconstruction data was studied in 7,8 on brain perfusion.

In this paper we extract the prior knowledge basis function set from liver CT perfusion reconstruction data. We use this basis function set for TST to reconstruct the simulated C-arm CT perfusion scan of animal liver. We compare perfusion maps of TST using prior knowledge basis constructed from two and three CT scans, perfusion maps of TST using analytical bases and perfusion maps of straightforward reconstruction to CT perfusion maps.

2. MATERIALS AND METHODS

2.1 Animal Experiments

The CT perfusion scans of three domestic pigs were acquired using SOMATOM Force CT after embolization. The iodinated contrast material used was Imeron 300. The right hepatic artery was embolized with tantalum-based embolization material (Onyx) and coils. The duration and contrast material injection details are given in Table 1.

Send correspondence hana.haseljic@ovgu.de

7th International Conference on Image Formation in X-Ray Computed Tomography,
edited by Joseph Webster Stayman, Proc. of SPIE Vol. 12304, 1230420
 · 0277-786X · doi: 10.1117/12.2646449

Table 1: Perfusion Scans Duration and Details of Contrast Material Injection

Scan	Duration [s]	Dose [ml]	Flow rate [ml/s]	Flow duration [s]	Volume [ml]
1	65.997	14.0	3.0	7.0	20.0
2	56.997	10.43	2.8	5.07	14.9
3	41.998	10.43	2.9	5.1	14.9

2.2 Simulation of C-arm CT perfusion scan

We simulate the C-arm CT data by reprojecting the CT volume as in 9. We reproject the Scan 3, see Table 1 with C-arm CT projector according the acquisition protocol of the experimental C-arm CT perfusion scans of the liver used in 5,6. The total scan time is divided in ten runs covering the ten rotations of 200° with 248 views with pause time 412.44 s between every two consecutive runs.

2.3 Prior Knowledge Extraction

Two prior knowledge basis function sets are extracted from CT perfusion scans. First is extracted from first two CT scans from Table 1 and the second one from all three by applying SVD on time attenuation curves (TAC) of voxels inside the organ regions as in 7. All bones, catheters if visible and surrounding organs were excluded. The CT scans were reconstructed using syngo CT VA50A software. The time-resolved volumes of each scan were interpolated across the time interval of shortest scan, see 9.

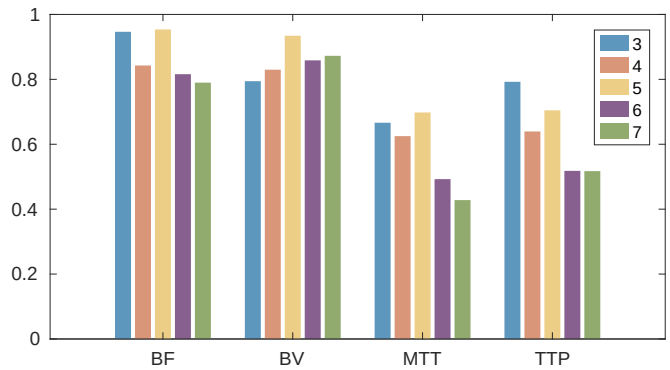

Figure 1: Pearson correlation coefficient with respect to CT ground truth perfusion maps reconstructed using basis function sets of different sizes.

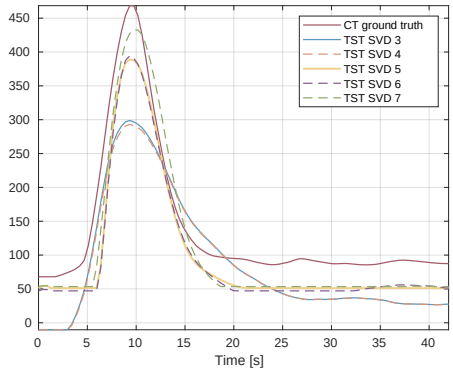

Figure 2: Arterial input function fitted using basis function sets of different size.

For the brain reconstruction it is recommended to use either three or five basis functions since more could cause instabilities in projections, see 10,11. In 6 five trigonometric functions formed the analytical basis function set. Based on the singular values, how well they fit the AIF and the Pearson correlation of perfusion maps with CT ground truth perfusion maps, we decide how many bases will form our basis function set, see Figures 1 and 2. By the means of the SVD our bases are orthonormal and therefore a suitable basis function set for TST. Our basis functions sets are shown in Fig. 3 and 4. The *Function 0* is a constant function and therefore left out from the graphs.

2.4 Time Separation Technique

The time separation technique, see 9,10, is a model-based reconstruction where the time attenuation development of every voxel is modeled as a linear combination of mutually orthonormal bases (1).

$$\mathcal{B} = \{\Psi_1, \ldots, \Psi_N\}. \tag{1}$$

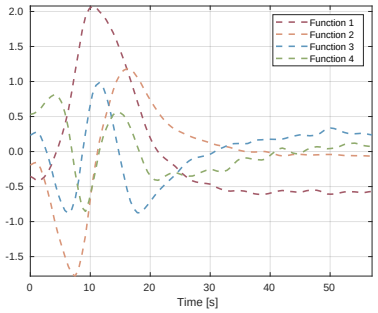

Figure 3: Extracted prior knowledge basis function set from two animals on the scan duration interval.

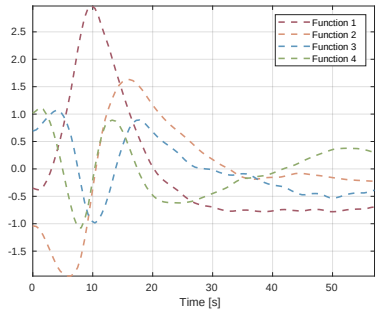

Figure 4: Extracted prior knowledge basis function set from three animals on the scan duration interval.

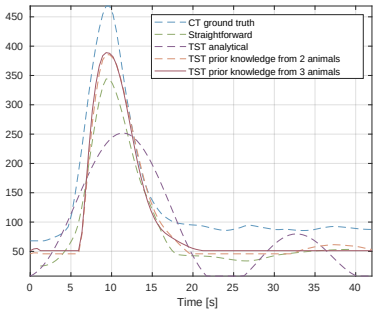

Figure 5: Arterial input function of CT ground truth, straightforward simulated C-arm CT and using analytical and prior knowledge basis sets.

The same way the pixels in projections can be modeled so the reconstruction problem $Ax = p$ becomes

$$A\sum_{i=1}^{N} w_{v,i}\psi_i(t) = \sum_{j=1}^{N} w_{p,j}\psi_j(t) \quad t \in \mathcal{I}. \tag{2}$$

where $\mathcal{I}$ is a vector of time points at which the volume was scanned. With scalar product of both sides with bases from $\mathcal{B}$ due to orthonormality of the bases, the reconstruction problem is reduced to N static reconstruction problems, see 9, 10, unlike the straightforward reconstruction where each rotation is reconstructed separately. The reconstruction is done using algebraic reconstruction developed and implemented within 8, 12. The voxel size is the same as in the CT scan $(x_v, y_v, z_v) = (0.7305, 0.7305, 1.5)$.

2.5 Perfusion Parameters Estimation

We calculate the perfusion parameters, blood flow (BF), blood volume (BV), mean transit time (MTT) and time to peak (TTP), using deconvolution technique, see 13. The time attenuation profile of every voxel is described as a convolution of AIF with the residual function. To determine the residual function the pseudoinverse with Tikhonov regularization is applied to Eq. (3).

$$\mathrm{tac(t)} = \mathrm{aif(t)} * f_r(\mathrm{t}). \tag{3}$$

For the calculation of the perfusion parameters, see Eq. (4), except for the TTP, it is important to select arterial input function (AIF) properly. This is not the case for the TTP which is estimated as the time from the beginning of the acquisition of the maximum value of the voxel's attenuation. The selected AIF for location $(x, y, z) = (194, 257, 65)$ is shown in Fig. 5.

$$BF = \max f_r(t), \quad BV = \sum_{i=1}^{n} f_r(\mathrm{i}), \quad MTT = \frac{BV}{BF}, \quad TTP = \arg\max_t f_r(t). \tag{4}$$

To avoid the possible instabilities of the BF we estimate the BF only based on the first 5 s of the acquisition as advised in 9. The perfusion maps are calculated using 14.

3. RESULTS AND DISCUSSION

We have simulated the C-arm CT perfusion scan and reconstructed it using model-based approach TST with prior knowledge basis function set as explained in previous section. First, we compare two prior knowledge basis function sets. In the basis function set generated from two animals we can observe the noise especially after the 15 s. In the basis function set extracted on three animals these instabilities are less pronounced, see Fig. 4.

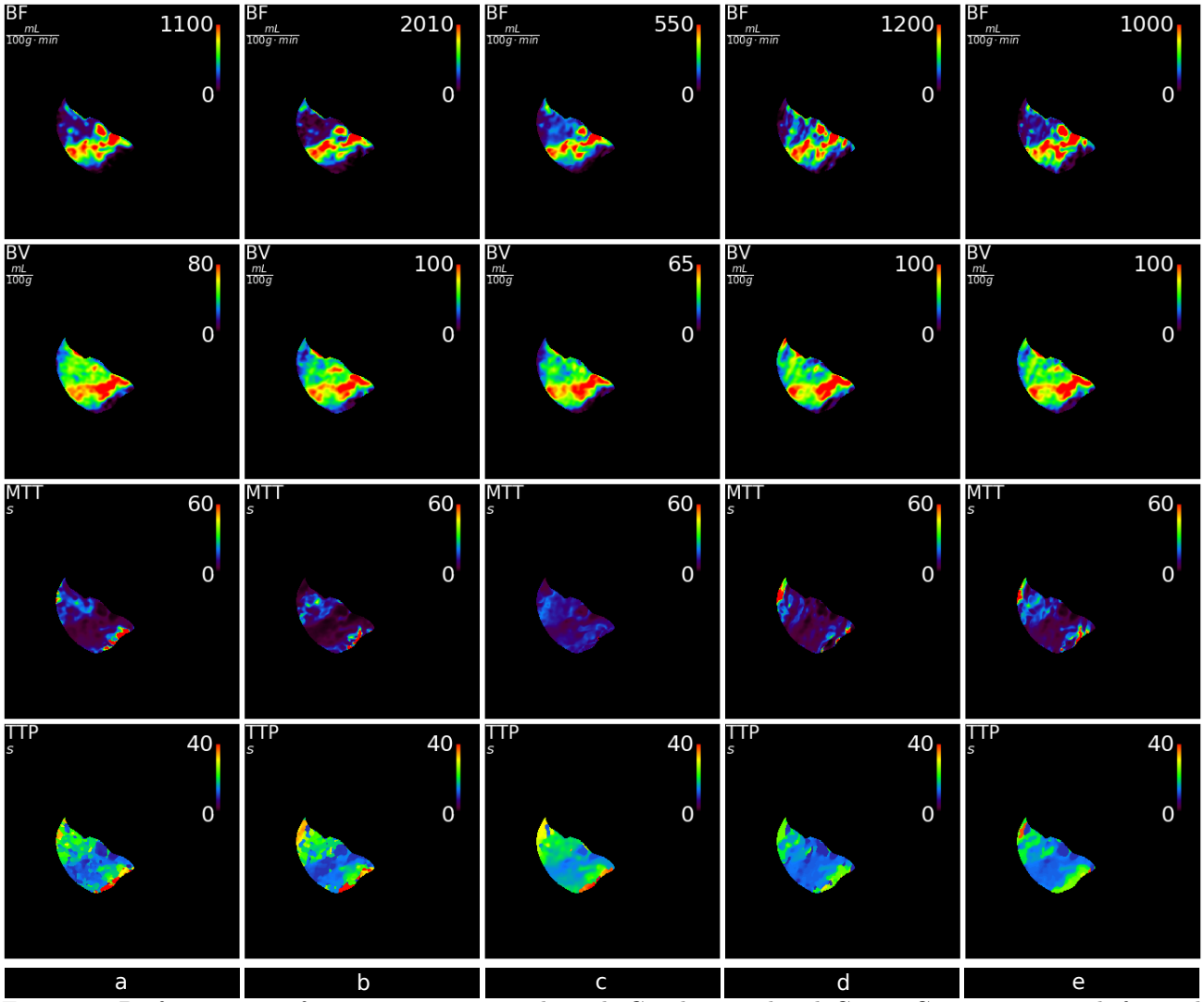

Figure 6: Perfusion maps for scan 3. a: ground truth CT, b: simulated C-arm CT scan - straightforward reconstruction, c: simulated C-arm CT scan - TST using five trigonometric basis, d: simulated C-arm CT scan - TST using prior knowledge basis extracted from two animals, e: simulated C-arm CT scan - TST using prior knowledge basis extracted from three animals.

However, both are fitting the AIF better than in straightforward approach and when fitted with trigonometric bases, see Fig. 5. It can be also observed that the *Function 1* from both basis function sets corresponds the AIF profile as the strongest pronounced signal. Note that all the values in AIF are lower due to introduced Gauss blur of 3.5 px.

The perfusion maps are shown in Fig. 6. The Pearson correlation coefficients and Normalized Root Mean Square Error (NRMSE) between the CT perfusion maps and simulated C-arm CT perfusion scans reconstructed by different means are given in Table 2.

In all perfusion maps it can be observed that the qualitative information is preserved. In perfusion images we use the *asist* color map, see 15. The lowest value in perfusion maps is dark blue. Hence, the dark blue area in BF and BV represents the embolized area. We can observe BF relative overestimation in TST with trigonometric basis and TST with prior knowledge extracted from two animals compared to ground truth. A relative underestimation is observed in straightforward approach.

Table 2: Pearson Correlation Coefficient and NRMSE in Respect to CT Ground Truth Perfusion Maps

Scan	BF	BV	MTT	TTP	BF	BV	MTT	TTP
Straightforward	0.9578	0.9528	0.7009	0.7741	0.1528	0.1101	0.2003	0.1725
TST analytic basis	0.9336	0.8837	0.4526	0.7921	0.1551	0.1404	0.3257	0.1886
TST SVD 2 animals	0.8898	0.8481	0.4779	0.5425	0.1786	0.1698	0.2728	0.2131
TST SVD 3 animals	0.9537	0.9344	0.6976	0.7045	0.1392	0.1242	0.2213	0.1823

From the correlation coefficients, see Table 2, the perfusion maps generated using prior knowledge extracted from three animals are more similar to ground truth than the perfusion maps using prior knowledge extracted from two animals. When compared to perfusion maps using analytical bases, the prior knowledge using three animals is better in all considering the normalized RMSE. The TST using prior knowledge generated with three animals is the second best.

The reason could be that the simulated CT scan is generated using CT and therefore better in terms of noise and sampling frequency compared to measurements of usual CBCT systems. Due to limited number of available CT perfusion scans of animal liver the same scan was used to simulate the C-arm CT perfusion data and to extract the prior knowledge. This, as well as the more scans involved in prior knowledge extraction, could have affected the better fitting of an AIF and better perfusion maps.

4. CONCLUSION

From the results we see that the model-based reconstruction by applying TST with prior knowledge bases is comparable to CT perfusion maps and it is better than the straightforward reconstruction for BF. We have also shown that it is possible to extract the bases using only two CT scans and to get perfusion maps comparable to CT ground truth. However, more scans should be used to extract the prior knowledge. In the future we will focus on studying if these results can be confirmed using real C-Arm CT datasets.

ACKNOWLEDGMENTS

This work was partly funded by the European Structural and Investment Funds (International Graduate School MEMoRIAL, project no. ZS/2016/08/80646) and the German Federal Ministry of Education and Research within the Research Campus STIMULATE, grant no. 13GW0473A and 13GW0473B).

REFERENCES

[1] Ogul, H., Kantarci, M., Genc, B., Pirimoglu, B., Cullu, N., Kizrak, Y., Yilmaz, O., and Karabulut, N., "Perfusion CT imaging of the liver: review of clinical applications," *Diagnostic and Interventional Radiology* **20**, 379–389 (aug 2014).

[2] Syha, R., Gatidis, S., Grözinger, G., Grosse, U., Maurer, M., Zender, L., Horger, M., Nikolaou, K., and Ketelsen, D., "C-arm computed tomography and volume perfusion computed tomography (VPCT)-based assessment of blood volume changes in hepatocellular carcinoma in prediction of midterm tumor response to transarterial chemoembolization: a single center retrospective trial," *Cancer Imaging* **16** (Sept. 2016).

[3] Mueller, K., Fahrig, R., Manhart, M., Deuerling-Zheng, Y., Rosenberg, J., Moore, T., Ganguly, A., and Kothary, N., "Reproducibility of parenchymal blood volume measurements using an angiographic c-arm CT system," *Academic Radiology* **23**, 1441–1445 (Nov. 2016).

[4] O'Donohoe, R. L., Kavanagh, R. G., Cahalane, A. M., Houlihan, D. D., McCann, J. W., and Ryan, E. R., "C-arm cone-beam CT parenchymal blood volume imaging for transarterial chemoembolization of hepatocellular carcinoma: implications for treatment planning and response," *European Radiology Experimental* **3** (May 2019).

[5] Datta, S., Müller, K., Moore, T., Molvin, L., Gehrisch, S., Rosenberg, J., Saenz, Y., Manhart, M., Deuerling-Zheng, Y., Kothary, N., and Fahrig, R., "Dynamic measurement of arterial liver perfusion with an interventional c-arm system," *Investigative Radiology* **52**, 456–461 (Aug. 2017).

[6] Haseljić, H., Kulvait, V., Frysch, R., Hensen, B., Wacker, F., Rose, G., and Werncke, T., "The Application of Time Separation Technique to Enhance C-arm CT Dynamic Liver Perfusion Imaging," in [*16th International Meeting on Fully Three-Dimensional Image Reconstruction in Radiology and Nuclear Medicine*], (2021).

[7] Eckel, C., Bannasch, S., Frysch, R., and Rose, G., "A compact and accurate set of basis functions for model-based reconstructions," *Current Directions in Biomedical Engineering* **4**, 323–326 (Sept. 2018).

[8] Kulvait, V. and Rose, G., "Software Implementation of the Krylov Methods Based Reconstruction for the 3D Cone Beam CT Operator," in [*16th International Meeting on Fully Three-Dimensional Image Reconstruction in Radiology and Nuclear Medicine*], (2021).

[9] Kulvait, V., Hoelter, P., Frysch, R., Haseljić, H., Doerfler, A., and Rose, G., "Time separation technique with the basis of trigonometric functions as an efficient method for flat detector CT brain perfusion imaging," *Submitted for consideration to Medical physics* (2021). Preprint at https://arxiv.org/abs/2110.09438.

[10] Bannasch, S., Frysch, R., Pfeiffer, T., Warnecke, G., and Rose, G., "Time separation technique: Accurate solution for 4D C-arm-CT perfusion imaging using a temporal decomposition model," *Medical Physics* **45**, 1080–1092 (feb 2018).

[11] Kulvait, V., Hoelter, P., and Doerfler, Arnd Rose, G., "Noise and dose reduction in CT brain perfusion acquisition by projecting time attenuation curves onto lower dimensional spaces," in [*SPIE Medical Imaging 2022*], (2021). accepted contribution.

[12] Kulvait, V., "Kct cbct a software package for algebraic ct reconstruction." https://github.com/kulvait/KCT{_}cbct (2021).

[13] Fieselmann, A., Kowarschik, M., Ganguly, A., Hornegger, J., and Fahrig, R., "Deconvolution-based CT and MR brain perfusion measurement: Theoretical model revisited and practical implementation details," *International Journal of Biomedical Imaging* **2011**, 1–20 (2011).

[14] Kulvait, V., "Kpct perfviz a software package for creating perfusion maps." https://github.com/kulvait/KPCT{_}perfviz (2021).

[15] Kudo, K., "Acute Stroke Imaging Standardization Group Japan recommended standard LUT (a-LUT) for perfusion color maps.." http://asist.umin.jp/data-e.shtml (2005). Accessed April 9, 2021.